Experimental investigation on optical spectral deformation of embedded FBG sensors

Xiaoxing Zhang, Jean-Joseph Max, Xuenian Jiang, Lucy Yu, Hassan Kassi
ITF Laboratories, Inc. 400 Montpellier Boulevard, Montreal, Quebec, Canada, H4N 2G7

ABSTRACT

With the rapid development of Fiber Bragg Grating (FBG) sensing during recent years, FBG sensors are used in many fields; applications involving impact and vibration measurement require a high-speed interrogator. We have developed and prototyped a high-speed FBG interrogation system with a sampling rate up to 5 kHz. We show that FBG sensor optical spectral deformation may affect the performance of interrogators, such deformation can be introduced from non-uniform strain field or during FBG sensor packaging. This paper reports the experimental investigation of the impacts of the FBG spectral deformation on the interrogator accuracy, sensors with different optical spectral shapes are tested and analyzed, furthermore, we show how this high-speed interrogator is more tolerant to such deformation than peak tracking instruments.

Keywords: Fiber Bragg grating, FBG sensor, interrogation, FBG interrogator, spectral deformation, strain field

1. INTRODUCTION

The fiber Bragg grating (FBG) has demonstrated its sensing property possessing advantages over other sensors for more than a decade, especially in high electromagnetic fields and hazardous environments the FBG sensor presents its superiority to other kinds of gauges. The high sensitivity, excellent reproducibility, and reliable stability are important features of FBG sensors. FBG sensors have been applied in varied kinds of applications, including civil engineering, geotechnology, oil and gas, damage detection, structural monitoring, and many more.

Basic principle of FBG interrogation generally uses wavelength scanning. The light source can be a narrow linewidth tunable laser or a wide-band light source covering the whole measurement band together with a tunable optical filter. The wavelength-scanning can be realized through scanning the wavelength of the laser or tuning the filter [1]. Recently several new technologies have been implemented in FBG interrogation systems [2,3,4]. However some of these technologies show speed limitations, making the interrogators suitable for static, long-term monitoring only. Some applications are now pursuing adopting large number of sensors to be detected with a single interrogation system. In such case, a large dynamic range is needed in order to compensate for fiber losses in installation and connection. To detect a large number of sensors simultaneously at high-speed is another challenge. Not all technologies can achieve high-speed interrogation and a large number of sensors.

Using a broadband light source to illuminate the FBG, part of light that obeys the Bragg condition is reflected and the rest of the light is transmitted. When an FBG undergoes a uniform strain along the grating, the FBG sensing principle becomes simply tracking the peak Bragg wavelength which shifts proportionally to the strain and temperature. However in a non-uniform strain field, the Bragg wavelength condition is more complicated. Consequently, the reflected FBG spectrum is not only shifted as in uniform strain field, but also broadened and even split into multiple peaks. In such a case, the Bragg wavelength is difficult to track. There are some papers involving fiber Bragg gratings in non-uniform strain field: Giaccari [5] and his group reported on the use of FBG to determine non-uniform internal strain. Their approach is to measure grating complex impulse response with optical low coherence reflectometer. The local Bragg wavelength is retrieved with layer-peeling technique. Peters et al [6] experimentally measured the response of an FBG to a non-homogenous strain.

To the best of our knowledge, this paper is the first report of the experimental investigation on different kinds of spectral deformation of embedded fiber Bragg grating sensors. We experimentally evaluate the measurement from the deformed FBGs.

2. CGT HIGH-SPEED INTERROGATOR

Among the FBG sensor interrogation mechanisms, the most widely used methods include wavelength scanning and various interferometric approaches [1,2,4]. For interrogating a large number of sensors, there are wavelength domain demultiplexing (WDM), time domain demultiplexing (TDM) with modulated light source, and hybrid technologies [2,3,4]. The wavelength interpretation can also be performed by different ways such as peak wavelength searching and tracking, curve fitting, and zero-crossing algorithms. Such interrogation technologies suffer from speed limitations, these limitations preclude their use for vibration, impact, and other dynamic measurements which require a high interrogation speed. ITF Labs has developed a CGT (Circulating Grating Transform) high-speed interrogator reaching up to 5kHz sampling rate. It has been successfully used in many experiments and studies in universities and laboratories.

Figure 1 displays the schematic diagram of the high-speed interrogator. A built-in broadband light source illuminates the FBG sensors. FBG reflected signal is split into two portions. One part of the light is integrated through a "linear" optical filter and the other simply integrated. The ratio between the two portions of signal is: (i) independent of light source fluctuation; (ii) related to FBG Bragg wavelength location. Figure 2 shows the transmission spectrum of an optical filter along with the grating sensor reflection spectrum at different strains. As the Bragg wavelength increases, the transmitted optical power decreases accordingly. Calibration of such measurement is not straight forward due to the integration over the relatively broad spectrum reflected by an FBG. We have developed an improved calibration method that permitted us to achieve a ±5pm accuracy in laboratory conditions. The instrument described here possesses no scanning or moving parts, therefore it is possible to realize high-speed interrogation [7]. A sampling rate of 5kHz has been reached, 100 kHz version is under development.

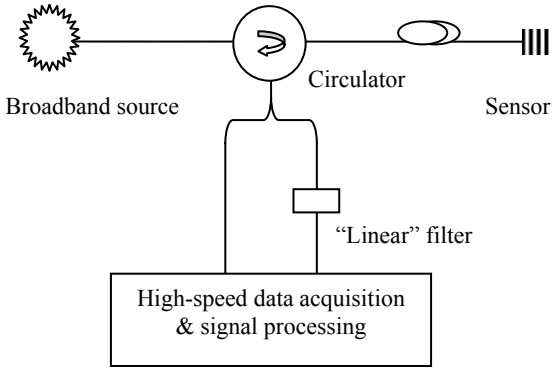

Figure 1. CGT high-speed interrogator schematics

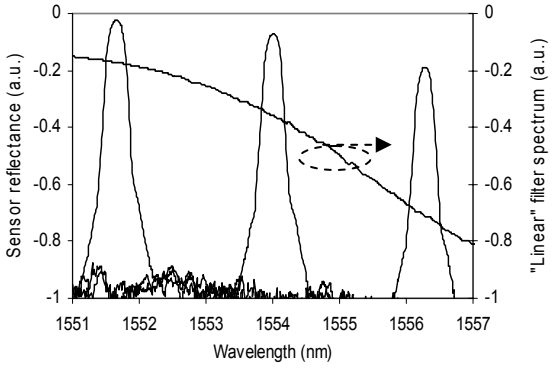

Figure 2. Wavelength shift converts into intensity change

3. STRAIN MEASUREMENT AND FBG SENSOR SPECTRAL DEFORMATION

3.1 Dynamic measurement

One of the major advantages of the CGT interrogator is its capability of dynamic measurement, with a CGT interrogator, various dynamic measurements have been made; Figure 3 shows one of the fatigue test results with an FBG strain sensor. A sinusoidal load was applied at a frequency of 2Hz, 100,000 cycles were tested of which 5 seconds are displayed. For comparison purpose, an electrical strain gauge was used on the same specimen, both FBG sensor and the strain gauge were glued on the same specimen symmetrically to the loading area; the electrical strain gauge sampling rate was 24 Hz (shown in diamonds), whereas CGT interrogator sampling rate was 333 Hz (shown in continuous line). The result shows that FBG interrogator and electrical strain gauge measurements are in good agreement. The obtained relation between FBG sensor wavelength and electrical strain gauge readout is 1.21±0.01pm/με. This agrees with the theoretical value (see Section 3.2).

Figure 4 is a frequency response test, the FBG sensor was glued onto a transducer (loud speaker), perpendicularly to the membrane in order that the membrane's movement directly induces fiber (and FBG) elongation, that is strain. A sinusoidal signal at 1kHz was applied to the transducer. The FBG response was obtained through CGT interrogator at 5 kHz sampling rate, for a duration of 1 second. The first 0.01 seconds data is shown in Figure 4 (dots). Each cycle follows well with the sinusoidal wave (continuous line). The frequency is accurately retrieved with CGT interrogator. Utilizing a custom Fast Fourier Transform (FFT) program the precise frequency is obtained. This shows that CGT interrogator is capable of measuring high-speed events.

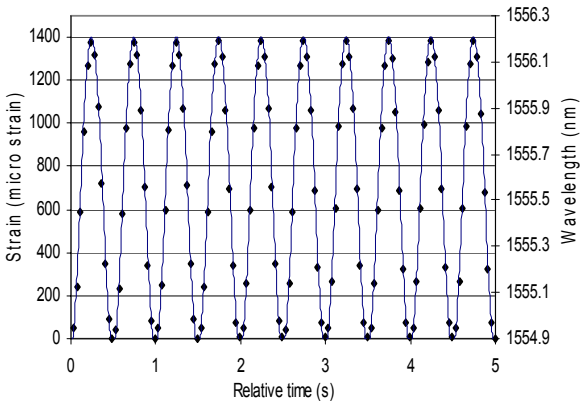

Figure 3. Fatigue test: comparison between FBG/ CGT interrogator (333Hz, line) and electrical strain gauge (24 Hz, diamonds)

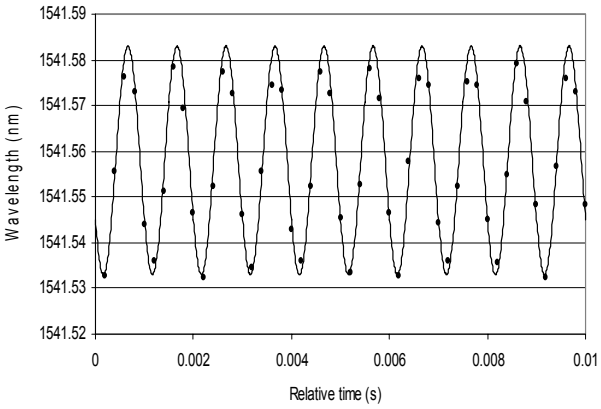

Figure 4. CGT interrogator frequency response. Signal Frequency: 1kHz.

3.2 FBG response to strain

During the experimental measurement with CGT interrogator, we found that the spectrum of FBG sensor may sometimes be deformed for different reasons. Such spectral deformation can result in measurement errors. It becomes one of the error sources of the interrogator. To improve the performance of CGT interrogator, it is worth investigating the spectral deformation of FBG sensors.

A basic assumption is made that uniform fiber Bragg grating acts following Bragg condition

$$\lambda_B = 2n_{eff}\Lambda \tag{1}$$

where n_{eff} is the effective refractive index of the grating, Λ is grating period, and λ_B is Bragg wavelength. Both changes of effective index and the grating period can cause Bragg wavelength shift. When such an FBG sensor is loaded under a uniform strain field, ideally, the Bragg wavelength is only shifted while the spectral shape of the FBG keeps unchanged with no deformation. Therefore measuring such wavelength shifts gives information related to the load.

Assuming temperature is constant, when a sensor is loaded in a uniform strain field, the relative Bragg wavelength shift can be given as [8]

$$\frac{\Delta\lambda_B}{\lambda_B} = (1 - p_e)\varepsilon_z \tag{2}$$

where p_e is the effective photoelastic coefficient (p_e = 0.22 for fused silica), ε_z is axial strain and $\Delta\lambda_B$ is Bragg wavelength shift. Hence, at Bragg wavelength of 1550 nm the calculated strain factor is 1.21 pm/με.

Under a non-uniform axial strain, the strain is a function of the position along the longitudinal axis of the FBG (z). Therefore the relative Bragg wavelength becomes [5]

$$\frac{\Delta\lambda_B(z)}{\lambda_B(z)} = (1 - p_e)\varepsilon_z(z) \tag{3}$$

In such a case, it is local Bragg wavelength shift that is related to the applied local strain.

3.3 Examples of FBG spectral deformation

FBGs are usually apodized with specifically designed function in order to suppress side lobes. Ideally, when loaded the FBG spectrum simply shifts. The wavelength shift is proportional to the load (no deformation occurs). However, in some situations, the FBG spectrum can be deformed, for example, under non-uniform strain. Figure 5-A shows the spectrum of an apodized FBG that was embedded in a material. Thin line displays without load and thick line shows with compression load. The spectral deformation is clearly seen. It is asymmetrically broadened, for such FBG sensors, the Bragg wavelength interrogation may produce errors when simply tracking the maximum of the spectrum.

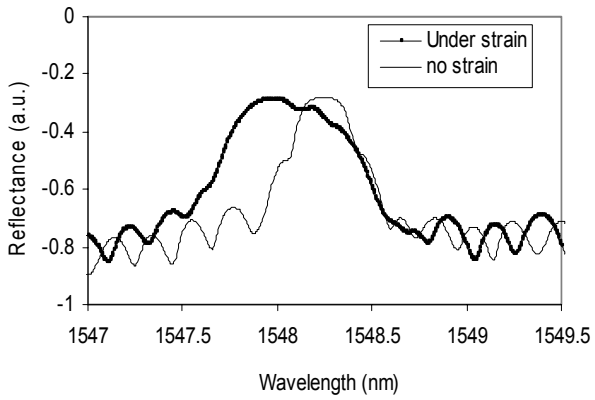

Figure 5-A

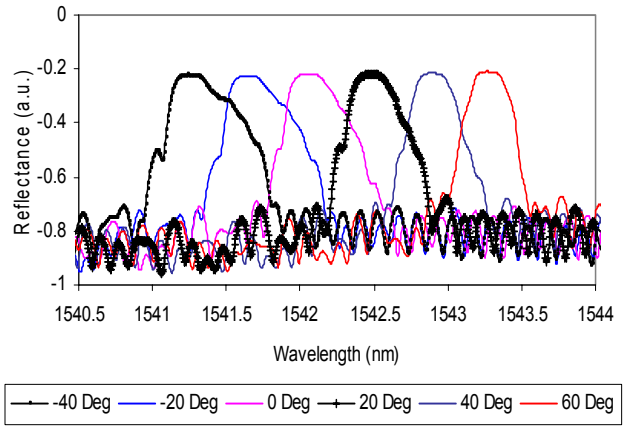

Figure 5-B

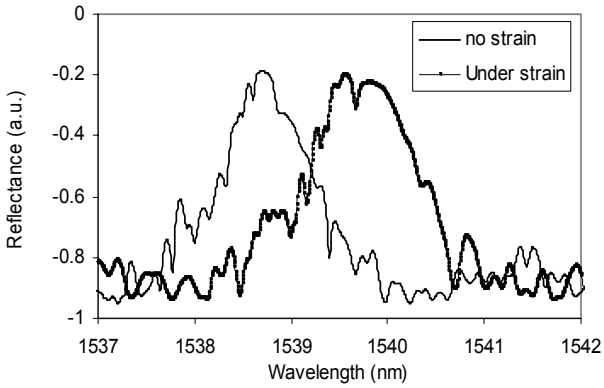

Figure 5-C

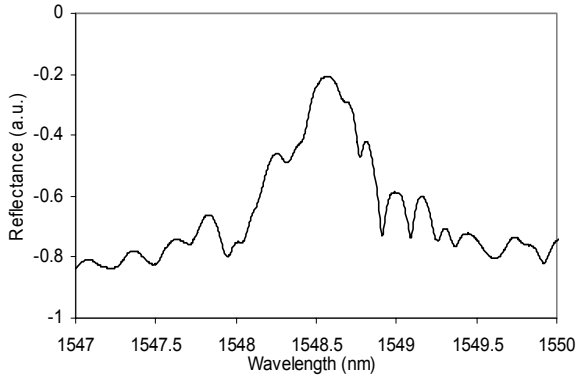

Figure 5 -D

Figure 5. Deformed FBG spectra

A second example demonstrates temperature dependent deformation of an embedded FBG that is subject to inducing by packaging. Figure 5-B shows the shifts and broadening of the spectrum under different temperatures from +60°C to -40°C. At 60°C, the FBG reflected spectrum is normal, decreasing temperature shifts the Bragg wavelength toward shorter wavelengths. At 20°C the spectrum is broadened and the side lobe level increases considerably, with further reduction in temperature, the spectrum is not only broadened but also asymmetrically deformed.

Another example is where the spectrum possesses multiple peaks which may even split further under load. Figure 5-C shows the spectra of an embedded FBG with and without strain applied. Without applying strain, the spectrum (thin line) shows two split peaks near the top, when a strain is applied, the spectrum is broadened and split further. In both cases interrogating such an FBG sensor could produce erroneous results.

An embedded FBG can also display spectral deformation at free status (no strain applied) if it is not suitable packaged. Figure 5-D shows such an example, although it has one unique peak, it is highly asymmetrical and shows reduced reflectivity.

3.4 Sources of FBG spectral deformation

The above examples show that there are several different types of spectral deformation. These deformations are caused by non-uniform strains in the embedded FBGs. For further investigation, we analyze two possible sources that can introduce such non-uniform strain. The first is FBG period chirp due to FBG bending, as shown in Figure 6, load applied at the middle of the grating can result in the bending of the FBG itself. In particular, long FBG suffers from such bending easily. When an FBG is bent, the middle and the ends of the grating undergo different strains, on the other hand, the traverse load leads to compression in the inner part of FBG and tension in the outer part, thus the strains are not uniform, leading to chirp of the period.

For a linear chirped FBG, the chirp in the period can be related to the chirped spectrum bandwidth $\Delta\lambda$ [9]

$$\Delta\lambda = 2n_{eff}(\Lambda_{Long} - \Lambda_{Short}) \tag{4}$$

where $\Delta\lambda$ is the chirped spectrum bandwidth of the grating, Λ_{Long} and Λ_{Short} are the longest and shortest period of chirped FBG, and n_{eff} is effective refractive index. Equation (4) can also be written as

$$\Delta\lambda = 2n_{eff}\Delta\Lambda_{chirp} \tag{5}$$

where $\Delta\Lambda_{chirp}$ is the total chirp of a chirped FBG. For a linear chirped grating of length L, the chirped bandwidth can also be expressed as

$$\Delta\lambda = 2n_{eff}L\delta \tag{6}$$

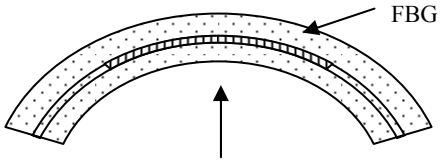

Figure 6. Long FBG chirped by bending

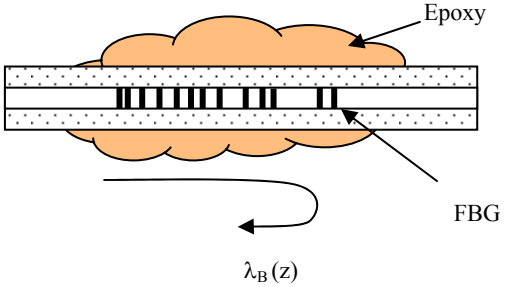

Figure 7. Embedded FBG chirped by epoxy

where δ is FBG chirp per unit length (usually nm/cm). It can be clearly seen that a chirped FBG can introduce wavelength broadening. If the chirp is not linear, the deformation of the spectrum is complicated, to reduce such deformation, it is recommended to use short FBGs.

Another source of FBG spectral deformation is from the epoxy used to glue FBG, non-homogenous epoxy applied onto the grating can restrain some parts of the grating locally and induce residual strain, as shown in Figure 7. This residual strain can create FBG local chirp and deforms the shape of FBG spectrum. It has been reported that the axial strain is related to the chirp distribution [5], equations (4)~(6) show that chirped FBG spectral bandwidth is a function of the chirp distribution, therefore, to retrieve the chirp one can deduce the axial strain and spectral bandwidth information. ITF Labs has studied the sensor spectral deformation and developed a special package procedure in order to minimize the spectral deformation of FBG sensors.

3.5 Impact on measurements

The spectral deformation of FBG sensors certainly affects the FBG measurement, from experiment we have found that the spectral deformation of the FBG sensor can sometimes lead to difficulties in tracking the Bragg wavelength, no matter what interrogation technology is used, consequently, the spectral deformation degrades the performance of the instrument, and can even be severe enough to make it fail to measure. We experimentally investigate the impact of the spectral deformation on CGT interrogator and other wavelength detecting instruments, and identify the capability of CGT interrogator comparing to other instruments.

To investigate the magnitude of this influence, several experiments were devised, in one of the experiments the spectral deformation was intentionally created with an embedded FBG. Pressure applied onto the grating was gradually increased. The deformation was designed to be increasingly more non-uniform as the load increased by making the fiber Bragg grating bent. Without any pressure applied, the grating spectrum appears normal; as the pressure (bending) applied to the FBG increases, the deformation is increased in turn. Figure 8 shows the measurement result of such deformed FBG sensor with Ando AQ6317B Optical Spectrum Analyzer (OSA) and CGT interrogator, respectively, starting from the pressure of 100,000 Pa. At low pressure (less than 100,000 Pa), the wavelengths obtained by the interrogator and OSA are in agreement. However when pressure is increased, the spectrum deforms more and becomes asymmetrically broader with multiple peaks, the resulting wavelengths from CGT interrogator and OSA differ notably.

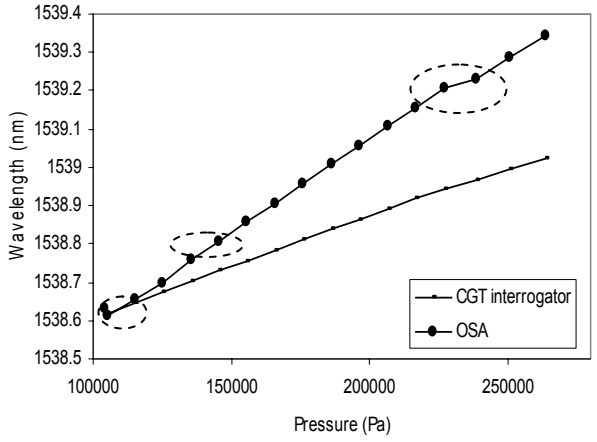

Figure 8. Measurement of a deformed FBG with OSA and CGT interrogator

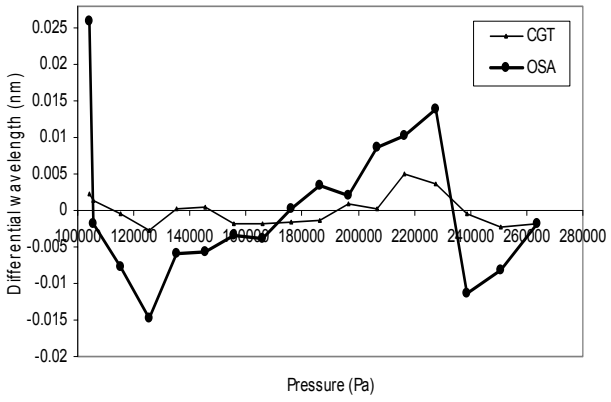

Figure 9. Comparison of measurement results from OSA and CGT interrogator

Experiment result shows that the relationship between wavelength obtained from OSA and pressure applied onto the FBG sensor is not properly continuous (Figure 8). The break observed in the OSA results is due to the peak splitting

close to the top of the grating spectrum. Such deformation affects the measurement of 3-dB central wavelength and leads to jumps (indicated in the circles). By comparison, the result from CGT interrogator shows a smooth and consistent result, utilizing fitting algorithm one can compare the difference between measured wavelength and calculated wavelength. Figure 9 shows the wavelength differences between the measured wavelength and fitted wavelength. There is considerable fluctuation on differential wavelength in the OSA measurement, while CGT interrogator measured wavelength is much better behaved.

4. CONCLUSION

This paper introduced the principle of CGT high-speed interrogator developed by ITF Labs. In order to improve the performance of CGT interrogator where noticeable sensor non-uniformity occurs, FBG sensor spectral deformation was investigated. Based on the experimental test results, several types of spectral deformations were discussed and analyzed. Further investigation revealed two predominant sources of FBG spectral non-uniformity that are introduced by FBG bending and the epoxy non-uniformity. From the experiments and analyses it is shown that the spectral bandwidth is related to FBG local chirp. This local chirp follows the axial strain applied on the FBG sensors. We also investigated the impact of the spectral deformation on measurements. The experiments show that deformed FBG can affect the continuity of the measurement on OSA or other instruments with peak tracking approach, while CGT interrogator can make more accurate measurement. This investigation shows that CGT interrogator is capable of both dynamic and static measurements with high accuracy even in the conditions of FBG undergoing non-uniform strain.

ACKNOWLEDGEMENT

The authors would like to acknowledge professor B. Benmokrane and his group in University of Sherbrook, Quebec, Canada, for performing fatigue tests with CGT high-speed interrogator.

REFERENCE

1. Alan D. Kersey et al., “Multiplexed fiber Bragg grating strain sensor system with a fiber Fabry–Perot wavelength filter,” Opt. Lett., vol. **18**, p. 1370, 1993.
2. Alan D. Kersey, Michael A. Davis, Heather J. Patrick, Michel LeBlanc, “Fiber Grating Sensors”, J. Lightwave Technol., vol. **15**, NO. 8, pp.1442-1463, 1997.
3. A Wilson, S W James and R P Tatam, “Time-division-multiplexed interrogation of fibre Bragg grating sensors using laser diodes”, Meas. Sci. Technol. vol. **12** pp. 181-187, 2001.
4. Abdeq M. Abdia and Alan Kost, “Infrastructure optics”, Smart Structures and Materials, Proc. SPIE vol. **5384** pp. 218-228, SPIE, Bellingham, WA, 2004.
5. Philippe Giaccari, Gabriel R Dunkel, Laurent Humbert, et al, “On a direct determination of non-uniform internal strain fields using fiber Bragg gratings”, Smart Mater. and Struct., vol **14**, pp.127-136, 2005.
6. Peters K, Pattis Ph, Botsis J, et al, “Experimental verification of response of embedded optical fiber Bragg grating sensors in non-homogenous strain fields”, J. Opt. Lasers Eng. vol.**33**, p. 107, 2000
7. Xiaoxing Zhang, Jean-Joseph Max and Hassan Kassi, “C+L band erbium-doped fiber ASE source enables high-speed FBG sensor interrogation”, Photonics North, Proc. SPIE vol. **6343**, Quebec city, Canada, 2006.
8. Seiji Kojima, Shinji Komatsuzaki, Yoshinori Kurosawa, Akihito Hongo, “Embedding type strain sensors using small diameter fiber Bragg grating to composite laminate structures”, Hitachi Cable Review, No.**23**, pp.11-15, 2004.
9. Raman Kashyap, *Fiber Bragg Gratings*, 1st ed., Academic Press, London, UK, 1999.